A domain decomposition method for quasi-incompressible formulation with discontinuous pressure fields

Pierre Gosselet, Christian Rey, Françoise Léné, Pascal Dasset

A domain decomposition method for quasi-incompressible formulations with discontinuous pressure field

Application to the mechanical study of a flexible bearing

P. Gosselet*, C. Rey*, F. Léné* and P. Dasset**

* Laboratoire de Modélisation et Mécanique des Structures,

FRE 2505 du CNRS, UPMC, 8 rue du Capitaine Scott, 75015 PARIS

** SNECMA Moteurs, 33187 Le Haillan

February 3, 2020

Abstract

We study the implementation of a domain decomposition method for structures with quasi-incompressible components. We chose a mixed formulation where the pressure field is discontinuous on the interfaces between substructures. We propose an extension of classical preconditioners to this class of problems. The numerical simulation of the mechanical behaviour of the flexible bearing of the nozzle of a solid propellant booster is then conducted using various Newton-Krylov parallel approaches. We present the main mechanical results and compare the numerical performance of the parallel approaches to a sequential approach.

Nous étudions la mise en oeuvre d'une méthode de décomposition de domaine pour structures à composants quasi-incompressibles. Une formulation mixte à champ de pression discontinu aux interfaces entre sous-structures est retenue ; nous proposons, pour cette classe de problèmes, une extension des préconditionneurs classiques. La mise en oeuvre de la simulation numérique du comportement mécanique d'une butée flexible de tuyère de propulseur à propergol solide par diverses approches parallèles itératives de type Newton-Krylov est alors proposée. Nous présentons les principaux résultats mécaniques ainsi que les performances numériques obtenues par les approches parallèles retenues et une approche séquentielle.

Keyword: Domain decomposition method, Newton-Krylov, quasi incompressibility, mixed formulation

Mots-clés Méthode de décomposition de domaine, Newton-Krylov, quasi incompressibilité, formulation mixte

1 Introduction

Primal and dual domain decomposition methods [6, 3] are among the first non-overlapping domain decomposition methods that have demonstrated numerical scalability with respect to both mesh and subdomain sizes. They have proved their efficiency on many types of problems such as second and fourth order linear (static and dynamic) elasticity, heterogeneous problems... and they are currently extended to other problems such as Stokes' equation [1].

In this paper we focus on the computation of quasi-incompressible elastomeric components using a primal domain decomposition method. Numerical simulation of the behaviour of such materials which main properties are the ability to handle large deformations, the non-linear behaviour and the quasi incompressibility, requires to use mixed displacement-pressure finite elements [6, 2]. More precisely we deal with the case of discontinuous pressure field on the interface of substructures and continuous or discontinuous pressure field inside substructures. Such an approach corresponds to any substructuration when the pressure is discontinuous between finite elements, and to physical decomposition between different pieces when the continuity of pressure is ensured inside substructures (e.g. interface between steel and elastomer or two different elastomeric pieces). However, as the incompressible/compressible heterogeneity is not taken into account in a satisfying way by current preconditioners, we extend them to this class of problems. Beside, because of non linearities, we use a non-linear solver leading to the solution to a sequence of ill-conditioned linear systems with both non invariant matrix and right-hand side. Various strategies to accelerate the solution to successive systems [9, 10, 11] have already been developed, and evaluated coupled with a dual domain decomposition method. We assess the performance of such Krylov acceleration approaches coupled with the primal domain decomposition method.

All numerical assessments relate to a very challenging industrial problem: the numerical simulation of steel-elastomer stratified structures. These structures are widely used in aerospace industry

to provide powerful elastic supports such as suspensions for aircraft engines, filtering supports for revolving machines, blade-rotor connections of helicopters, rocket-nozzle connections of the Ariane V launcher. They may take the form of a flexible steel-elastomer structure located between the body and the nozzle of a solid propellant booster, of which the engine of the powder acceleration stages of the Ariane V launcher is a typical example.

Thus, we present in section (2) the formulation of the problem and the generic algorithms to achieve the simulation. We give in section (3) the extension of traditional preconditioners to the quasi-incompressible case and in section (4) a Krylov acceleration technique to solve the sequence of linear systems resulting from the linearization of the non-linear problem. In section (5) we present the flexible bearing which supports the assessments, and associated mechanical results; section (6) sums up numerical performance. Section (7) concludes this article.

2 Overview of the models and methods

2.1 Lagrangian formulation

We consider the computation of the equilibrium position of a body Ω made up of a quasi-incompressible hyperelastic material undergoing large deformation. We choose a lagrangian formulation where all variables are defined in the reference configuration. Let f denote the body force, g the surface traction imposed on $\partial_g\Omega$, u_0 the imposed displacement on the complementary part of the boundary. Taking into account the incompressibility leads to the introduction of an unknown pressure field p. The research of the equilibrium of the body (dead loading assumption) is equivalent to the research of the saddle point of the following lagrangian:

$$\begin{gathered}(u,p) \in (\{u_0\}+\mathcal{H}) \times \mathcal{P} \\ \mathcal{L}(u,p) = \int_\Omega \mathcal{W}(F)d\Omega + \int_\Omega p(h(J) - \frac{1}{2K}p)d\Omega - \int_\Omega fud\Omega - \int_{\partial_g\Omega} gudS\end{gathered} \tag{1}$$

The problem then reads:

$$\begin{gathered}\text{Find } (u,p) \in (\{u_0\}+\mathcal{H}) \times \mathcal{P} \ / \ \forall (v,q) \in \mathcal{H} \times \mathcal{P}, \\ \int_\Omega \frac{\partial \mathcal{W}}{\partial F}(Id+\nabla u) : \nabla v d\Omega + \int_\Omega ph'(J)\frac{\partial J}{\partial F} : \nabla v d\Omega = \int_\Omega fvd\Omega + \int_{\partial_g\Omega} gvdS \\ \int_\Omega (h(J) - \frac{1}{K}p)qd\Omega = 0\end{gathered} \tag{2}$$

Where $\mathcal{H}$ and $\mathcal{P}$ are the spaces of admissible displacement and pressure fields, F is the gradient of the deformation ($F = Id + \nabla u$, $J = \det(F)$), K is the compressibility modulus of the material. Free energy $\mathcal{W}(F)$ can be chosen from different models ([12, 5]). For isotropic materials, it is often written as a function of the $C = F^T F$ tensor invariants $\mathcal{W}(F) = \bar{\mathcal{W}}(I_1, I_2, J)$ where $I_1 = \mathrm{Tr}(C)$ and $I_2 = \frac{1}{2}(\mathrm{Tr}^2(C) - \mathrm{Tr}(C^2))$. Among others we cite the Mooney-Rivlin model:

$$\bar{\mathcal{W}}(I_1, I_2) = \frac{C_{10}}{2}(I_1 - 3) + \frac{C_{01}}{2}(I_2 - 3)$$

Where C_{01} and C_{10} are constants that characterize the material. Function $h(J)$ can also be given by various models, in the simplest case (linear model) $h(J) = (J-1)$.

The numerical solution to this variational problem is classically conducted using the finite element method. Subspaces $\mathcal{H}$ and $\mathcal{P}$ are replaced with finite dimension subspaces $\mathcal{H}_h \subset \mathcal{H}$ and $\mathcal{P}_h \subset \mathcal{P}$. Let us underline that the construction of mixed finite elements must in particular comply with compatibility conditions (Ladyzenska-Babuska-Brezzi condition [2]) thus restricting the possible choices of approximation spaces. However common choices for 3D problems are the $Q_2 - P_1$ hexahedral element (27 displacement nodes, 4 pressure nodes) and the $Q_2 - Q_1$ hexahedral element (20 displacement nodes, 8 pressure nodes).

2.2 Newton-type algorithms

The problem arising from the finite element method is nonlinear, let us write it $\mathcal{F}(x) = 0$ with $x = (u_h, p_h)$. The principle of Newton's algorithms is to build a sequence of linear systems the solutions of which converge to the solution to the non-linear problem. There are many versions of Newton's algorithms, the most widely used is Newton-Raphson's. This last method consists in iteratively substituting the solution to the equation $\mathcal{F}(x) = 0$ for its first order limited development around x^k:

$$\mathcal{F}(x^k) + \frac{d\mathcal{F}(x^k)}{dx}(x^{k+1} - x^k) = 0 \tag{3}$$

Newton-Raphson's method is known to converge fast when properly initialized. A very common extension is the incremental algorithm which consists in defining "steps of loading" and finding the

solution to the intermediate problems corresponding to these steps using the solution to the previous step as an efficient initialization. The linear system arising from Newton-Raphson's linearization reads:

$$\left(\begin{array}{cc} K_{uu} & K_{up} \\ K_{up}^T & K_{pp} \end{array} \right) \left(\begin{array}{c} v^k \\ q^k \end{array} \right) = \left(\begin{array}{c} f_u \\ f_p \end{array} \right) \text{ with } \left\{ \begin{array}{l} v^k = u^{k+1} - u^k \\ q^k = p^{k+1} - p^k \end{array} \right. \tag{4}$$

$$\begin{aligned}
\Big(K_{uu}(u^k,p^k)\Big)_{ij} &= \int_\Omega \left(\frac{\partial^2 \mathcal{W}}{\partial F^2} : \nabla\Phi_i \right) : \nabla\Phi_j d\Omega \\
&\quad + \int_\Omega p^k h''(J) \left(\frac{\partial J}{\partial F} : \nabla\Phi_i \right) \left(\frac{\partial J}{\partial F} : \nabla\Phi_j \right) d\Omega \\
&\quad + \int_\Omega p^k h'(J) \left(\frac{\partial^2 J}{\partial F^2} : \nabla\Phi_i \right) : \nabla\Phi_j d\Omega \\
\Big(K_{up}(u^k,p^k)\Big)_{ib} &= \int_\Omega h'(J) \left(\frac{\partial J}{\partial F} : \nabla\Phi_i \right) \Psi_b d\Omega \\
\Big(K_{pp}(u^k,p^k)\Big)_{ab} &= -\frac{1}{K} \int_\Omega \Psi_\alpha \Psi_\beta d\Omega \\
\Big(f_u(u^k,p^k)\Big)_i &= \int_\Omega f\Phi_i d\Omega + \int_{\partial_g\Omega} g\Phi_i dS - \int_\Omega \frac{\partial \mathcal{W}}{\partial F} : \nabla\Phi_i d\Omega \\
&\quad - \int_\Omega p^k h'(J) \frac{\partial J}{\partial F} : \nabla\Phi_i d\Omega \\
\Big(f_p(u^k,p^k)\Big)_a &= -\int_\Omega \Psi_\alpha \left(h(J) - \frac{1}{K} p^k \right) d\Omega
\end{aligned} \tag{5}$$

Where functions (Φ_i) and (Ψ_α) are the basis of the displacement and pressure fields. For a more complete description of Newton's type algorithm for incompressible non-linear elasticity, readers can refer to [7].

Remark: When using domain decomposition methods, because of insufficient Dirichlet's conditions or internal mechanisms, the stiffness matrix of some substructures may be not invertible; the computation of the kernel of the matrix is then an important point. As far as we know, there are no general results which indicate a priori the composition of the kernel. What can be demonstrated for substructures without mechanism is that the first system is the linearized elasticity system, then the vectors of the kernel are (rigid body displacements, zero pressure), for following systems vectors composed by (admissible translations, zero pressure) always belong to the kernel. We have never observed other kinds of null space modes (translations and rotations for the first system, only translations for the following systems). So we propose to use a geometrical computation of the rigid body motions for the first system and just suppress the rotations for the following systems.

Due to the inversibility of the K_{pp} submatrix, pressure nodes can be eliminated from the resolution process using a Schur condensation. One can solve the following system for the displacement unknown and compute pressure as post-process:

$$\tilde{K} v^k = \tilde{f} \text{ with } \left\{ \begin{array}{l} \tilde{K} = K_{uu} - K_{up} K_{pp}^{-1} K_{up}^T \\ \tilde{f} = f_u - K_{up} K_{pp}^{-1} f_p \end{array} \right. \tag{6}$$

In the case where there are no nodes on the interelement boundary (discontinuous pressure field) which is the case of the $Q_2 - P_1$ hexahedral element, this condensation is usually achieved at the element scale at a very low cost since the (Ψ_α) functions can be chosen orthonormal and then $K_{pp} = -\frac{1}{K} I_d$.

2.3 Primal domain decomposition method

We briefly recall the primal domain decomposition method [6] in a generic case, the next section focuses on its extension to mixed displacement-pressure formulations. We consider the discretized problem (4). Let us make a non-overlapping conform partition of discretized domain Ω into N subdomains $(\Omega^{(s)})_{1 \leqslant s \leqslant N}$, the interface of a subdomain is defined as $\Upsilon^{(s)} = \partial\Omega^{(s)} \backslash \partial\Omega$, the complete interface Υ is the union of the interfaces of all substructures.

Using classical notation (i stands for internal degree of freedom, b for boundary degree of freedom), the stiffness matrix of the s^{th} subdomain reads:

$$K^{(s)} = \left(\begin{array}{cc} K_{ii}^{(s)} & K_{ib}^{(s)} \\ K_{bi}^{(s)} & K_{bb}^{(s)} \end{array} \right) \tag{7}$$

The primal approach simply consists in eliminating internal degrees of freedom from the complete problem which can be done independently on each substructure constructing the local primal Schur complement $S_1^{(s)}$. Let u be the displacement field of the interface degrees of freedom, the problem to solve then reads:

$$Su = b \text{ with } \left\{ \begin{array}{c} S = \sum_s B^{(s)} S_1^{(s)} B^{(s)^T} \qquad b = \sum_s B^{(s)} b^{(s)} \\ S_1^{(s)} = K_{bb}^{(s)} - K_{bi}^{(s)} K_{ii}^{(s)^{-1}} K_{ib}^{(s)} \\ b^{(s)} = f_b^{(s)} - K_{bi}^{(s)} K_{ii}^{(s)^{-1}} f_i^{(s)} \end{array} \right. \tag{8}$$

The $B^{(s)}$ matrix projects the local interface $\Upsilon^{(s)}$ on the global interface Υ. For the primal approach, opposite to the classical dual method (FETI), crosspoints (points shared by more than 2 substructures) are not repeated when describing Υ.

Due to the existence of efficient preconditioners, system (8) is solved using a Krylov iterative solver (Conjugate gradient, GMRes...) which is well suited to the parallel architecture of modern computers. The Neumann preconditioner consists in approximating the inverse of the sum of local Schur complements by the sum of the inverse of local Schur complements. Let M^{-1} be the preconditioner:

$$\begin{aligned} M^{-1} &= \sum_s D^{(s)} B^{(s)} S_2^{(s)} B^{(s)^T} D^{(s)} \\ S_2^{(s)} &= S_1^{(s)^+} = \beta^{(s)} K^{(s)^+} \beta^{(s)^T} \end{aligned} \tag{9}$$

$\beta^{(s)} = (0_i \ Id_b)$ extracts from vectors defined on the subdomain $\Omega^{(s)}$ their trace on their interface $\Upsilon^{(s)}$. $K^{(s)^+}$ is a pseudo-inverse of matrix $K^{(s)}$, $S_2^{(s)}$ is the local dual Schur complement. $D^{(s)}$ is a diagonal scaling matrix ($\sum D^{(s)} = Id_\Upsilon$). When dealing with homogeneous structures, $D^{(s)}$ can be chosen equal to the inverse of the multiplicity of each degree of freedom. For heterogeneous structures [13], scaling has to provide information about the difference of stiffness between subdomains, most often this item of information is extracted from the diagonal of the $K_{bb}^{(s)}$ matrix:

$$D_i^{(s)} = \frac{(B^{(s)} \operatorname{Diag}(K_{bb}^{(s)}) B^{(s)^T})_i}{(\sum_k B^{(k)} \operatorname{Diag}(K_{bb}^{(k)}) B^{(k)^T})_i} \tag{10}$$

To become scalable with respect to the number of substructures, the primal approach equipped with the Neumann preconditioner has to be enriched with a coarse problem. The idea is to ensure that vectors that are multiplied by generalized inverse matrices $K^{(s)^+}$ belong to the image of $K^{(s)}$. This method is reported as balancing method [8] because its mechanical interpretation is to ensure the equilibrium of each substructure face up to rigid-body loadings. Noting r the residual ($r = b - Su$), preconditioning consists in computing $M^{-1}r$.

$$\begin{aligned} M^{-1}r = & \sum_s D^{(s)} B^{(s)} \beta^{(s)} K^{(s)^+} \beta^{(s)^T} B^{(s)^T} D^{(s)} r \\ & \forall s \ \beta^{(s)^T} B^{(s)^T} D^{(s)} r \in \operatorname{Im}(K^s) \\ \Leftrightarrow \quad & \forall s \ R^{(s)^T} \beta^{(s)^T} B^{(s)^T} D^{(s)} r = 0 \text{ with } \operatorname{Span}(R^{(s)}) = \operatorname{Ker}(K^{(s)}) \\ \Leftrightarrow \quad & \forall s \ (D^{(s)} B^{(s)} \beta^{(s)} R^{(s)})^T r = 0 \\ \Leftrightarrow \quad & G^T r = 0 \text{ with } G = \begin{pmatrix} \dots & D^{(s)} B^{(s)} \beta^{(s)} R^{(s)} & \dots \end{pmatrix} \end{aligned} \tag{11}$$

This condition is imposed using a proper initialization ($u_0 = G(G^T S G) G^T b$) and a projector $P = Id - G(G^T S G)^{-1} G^T S$; the preconditioner then reads PM^{-1}.

3 Extension of primal domain decomposition method to quasi-incompressible material with discontinuous pressure field

In this paper we deal with the case of discontinuous pressure fields at the interface of substructures. The pressure field inside substructures may be either continuous (e.g. hexahedral $Q_2 - Q_1$) or not (e.g. hexahedral $Q_2 - P_1$). In the case of continuous pressure field inside substructure, such a model corresponds to physical decompositions between stuck pieces (whatever their material may be, e.g. interface between steel and elastomer or two different elastomers or two different pieces of the same elastomer). Hence all pressure degrees of freedom are considered internal.

For the following equations i and b stand for internal and boundary displacement degree of freedom, p for pressure degree of freedom. Since pressure is considered as an internal field, the condensation shown in (6) can be realized at the substructure scale (if not yet realized at the element scale) without modifying the global problem. The interface problem then reads:

$$\tilde{S}u = \tilde{b} \text{ with } \begin{cases} \tilde{S} = \sum_s B^{(s)} \tilde{S}_1^{(s)} B^{(s)^T} & \tilde{b} = \sum_s B^{(s)} \tilde{b}^{(s)} \\ \tilde{S}_1^{(s)} = \tilde{K}_{bb}^{(s)} - \tilde{K}_{bi}^{(s)} (\tilde{K}_{ii}^{(s)})^{-1} \tilde{K}_{ib}^{(s)} & \\ \tilde{b}^{(s)} = \tilde{f}_b^{(s)} - \tilde{K}_{bi}^{(s)} (\tilde{K}_{ii}^{(s)})^{-1} \tilde{f}_i^{(s)} & \end{cases} \tag{12}$$

The expression of the matrices and vectors above is the expansion of equation (6):

$$\begin{pmatrix} \tilde{K}_{ii}^{(s)} & \tilde{K}_{ib}^{(s)} \\ \tilde{K}_{bi}^{(s)} & \tilde{K}_{bb}^{(s)} \end{pmatrix} = \begin{pmatrix} K_{ii}^{(s)} - K_{ip}^{(s)} K_{pp}^{(s)^{-1}} K_{pi}^{(s)} & K_{ib}^{(s)} - K_{ip}^{(s)} K_{pp}^{(s)^{-1}} K_{pb}^{(s)} \\ K_{bi}^{(s)} - K_{bp}^{(s)} K_{pp}^{(s)^{-1}} K_{pi}^{(s)} & K_{bb}^{(s)} - K_{bp}^{(s)} K_{pp}^{(s)^{-1}} K_{pb}^{(s)} \end{pmatrix}$$

$$\begin{pmatrix} \tilde{f}_i^{(s)} \\ \tilde{f}_b^{(s)} \end{pmatrix} = \begin{pmatrix} f_i^{(s)} - K_{ip}^{(s)} K_{pp}^{-1} f_p^{(s)} \\ f_b^{(s)} - K_{bp}^{(s)} K_{pp}^{-1} f_p^{(s)} \end{pmatrix} \tag{13}$$

Note above all that the resulting stiffness scaling $\tilde{D}^{(s)}$ is built from the diagonal $\tilde{K}_{bb}^{(s)}$, that is to say from the diagonal of the matrix $(K_{bb}^{(s)} - K_{bp}^{(s)} {K_{pp}^{(s)}}^{-1} K_{pb}^{(s)})$.

However if we do not condense the pressure, we have:

$$K^{(s)} = \begin{pmatrix} \begin{pmatrix} K_{ii}^{(s)} & K_{ip}^{(s)} \\ K_{pi}^{(s)} & K_{pp}^{(s)} \end{pmatrix} & \begin{pmatrix} K_{ib}^{(s)} \\ K_{pb}^{(s)} \end{pmatrix} \\ \begin{pmatrix} K_{bi}^{(s)} & K_{bp}^{(s)} \end{pmatrix} & K_{bb}^{(s)} \end{pmatrix} \tag{14}$$

$$Su = b \text{ with } \begin{cases} S = \sum_s B^{(s)} S_1^{(s)} {B^{(s)}}^T \qquad b = \sum_s B^{(s)} b^{(s)} \\ S_1^{(s)} = K_{bb}^{(s)} - \begin{pmatrix} K_{bi}^{(s)} & K_{bp}^{(s)} \end{pmatrix} \begin{pmatrix} K_{ii}^{(s)} & K_{ip}^{(s)} \\ K_{pi}^{(s)} & K_{pp}^{(s)} \end{pmatrix}^{-1} \begin{pmatrix} K_{ib}^{(s)} \\ K_{pb}^{(s)} \end{pmatrix} \\ b^{(s)} = f_b^{(s)} - \begin{pmatrix} K_{bi}^{(s)} & K_{bp}^{(s)} \end{pmatrix} \begin{pmatrix} K_{ii}^{(s)} & K_{ip}^{(s)} \\ K_{pi}^{(s)} & K_{pp}^{(s)} \end{pmatrix}^{-1} \begin{pmatrix} f_i^{(s)} \\ f_p^{(s)} \end{pmatrix} \end{cases} \tag{15}$$

Note that scaling matrix $D^{(s)}$ associated to the non-condensed pressure problem is then directly built from the $K_{bb}^{(s)}$ matrix.

Both problems (whether the pressure is condensed or not) are equal: $\tilde{S} = S, \tilde{b} = b$. It is then abnormal that scaling matrices should differ $\tilde{D}^{(s)} \neq D^{(s)}$. In fact the condensation of the pressure nodes leads to an overestimation of the stiffness; we then propose two different scalings which work fine whether the materials are compressible or not. The first one is built from the $K_{bb}^{(s)}$ diagonal (before condensation). Since obtaining this information may not be easy when using element-scale condensation, we propose a second scaling, simpler but even better, which is based on the shearing modulus μ of the different materials $D_j^{(s)} = \frac{\mu_j^{(s)}}{\sum_k \mu_j^{(k)}}$.

Table (1) summarizes the performance of the different scalings for the industrial structure described section (5). The element used is an hexahedra $Q_2 - P_1$ (27 displacement nodes, 4 internal pressure nodes). The new scalings show their efficiency, they even manage to achieve better results than the computation of the homogeneous structure. The effect of the perturbation $(-K_{bp}^{(s)} {K_{pp}^{(s)}}^{-1} K_{pb}^{(s)})$ introduced by the condensation can be observed on the usual stiffness scaling: the perturbation is bigger for the second system then it requires much more iterations to converge.

Decomposition	Type of scaling	Number of iterations	
		First system	Second system
6a-1r (6 proc.)	Topological	290	> 1000
6a-1r (6 proc.)	Usual stiffness ($\tilde{D}$)	120	726
6a-1r (6 proc.)	Stiffness before condensation	48	44
6a-1r (6 proc.)	Shearing modulus	43	39
6a-1r (6 proc.)	Homogeneous structure	93	116

Table 1: Action of the scaling - mixed element $Q_2 - P_1$

Remark: Of course, the same analysis can be conducted from the dual domain decomposition method (FETI algorithm). New dual scalings can be defined on the basis of the same principle, they proved similar efficiency.

4 Krylov acceleration strategy: GIRKS

The context of the study is the resolution of a succession of linear systems, let us consider the solving of the $(k+1)^{th}$ system $S^{k+1}u^{k+1} = b^{k+1}$, the aim of the following strategy is to reuse the information generated during the resolution of previous systems to solve the current system. The resolution of a linear system with a Krylov iterative solver leads to the construction of at least one basis W^{k+1} of the Krylov subspace for which the $\Gamma^{k+1} = {W^{k+1}}^T S^{k+1} W^{k+1}$ matrix is easily invertible. In the case of a Conjugate Gradient, note that W^{k+1} is then the set of research directions and Γ^{k+1} a diagonal matrix.

The GIRKS algorithm is a generalization of augmented Krylov subspace methods for multiple right hand sides [14] to the case of non-invariant matrices (multiple left hand sides). It has two distinct actions, first an initialization IRKS and a correction of the preconditioner GKC.

The IRKS algorithm (Iterative reuse of Krylov subspaces [11]) is based upon an iterative approach making it possible to evaluate at low cost a relevant initialization of a linear system with respect to previously generated Krylov subspaces. Once the initialization stage is complete, the algorithm is subject to a restarting procedure which can be considered as a Conjugate Gradient algorithm augmented with the Krylov subspace generated during the initialization stage. The GKC (Generalized

Krylov Correction [9]) algorithm corrects the preconditioner, solving approximatively an optimal preconditioning problem.

Figure (4) gives the complete algorithm of projected preconditioned conjugate gradient with GIRKS acceleration.

5 Study of the flexible bearing

5.1 Description

The orientation of the nozzle of a booster is achieved with a flexible bearing. This bearing is a stratified structure with thin spherical steel and elastomer layers, it is maintained by two metallic supports. The flexible bearing we study (fig. 2) was proposed by SNECMA Moteurs, it was designed to let the buckling of steel layers appear. This buckling was observed when performing an experimental study of the solid propellant booster of Ariane 5 rocket.

The structure is clamped on one external ring, a radial displacement imposed on one point at the bottom of the nozzle models the turning loading (5 degrees), a 4 MPa pressure due to the gases is imposed at the top of the flexible bearing (fig. 3). The resolution is conducted in two steps: first the turning problem is solved using two nonlinear increments (10 linear systems), then the compression problem is solved with 4 nonlinear increments (37 linear systems) or 10 nonlinear increments (48 linear systems) whether we want the buckling to appear or not.

Resulting from the identification of the materials, simple constitutive laws were chosen. Steel is defined using a Saint-Venant–Kirchoff model (Young modulus $E = 2.10^5$ MPa, Poisson's coefficient $\nu = 0.3$). Nearly incompressible elastomer is defined using a Mooney-Rivlin elastic potential ($C_{10} = 0.2$ MPa, $C_{01} = 0.$ MPa, $K = 2000$ MPa).

Many difficulties arise when carrying out the numerical simulation of this flexible bearing, first non-linearities due to the large strains, the instabilities and the behaviour of the elastomer, second, the high heterogeneities (5 degrees of magnitude separate the shearing moduli) and last the large and massive aspect of this 3D problem. The simulation is conducted using a Q_2 hexahedral finite element (20 displacement nodes) for steel and a $Q_2 - Q_1$ hexahedral finite element (20 displacement nodes, 8 pressure nodes) for elastomer, which leads to 75900 degrees of freedom.

5.2 Mechanical results

According to experimental results, the buckling is computed under a 3 MPa pressure. Buckling causes bifurcations of the displacement of some points (fig. 5, 6).

5.3 Decompositions used for the parallel simulation

The geometry of the structure is axisymmetric (while the loading is not). Substructures are hand-made decomposing either the axial section or the rotation. The nomenclature of a decomposition reads Na-Mr where N stands for the number of substructures in the axial section, M for the number of substructures in the rotation.

In the case of rotation-decomposed substructures, pressure is discontinuous at the elastomer/elastomer interface and continuous inside substructures. However, mechanical results are identical whatever the decomposition.

6 Numerical results

All computations presented here were realized on the SGI ORIGIN 2000 of the Pôle de Calcul Paris Sud. We compare performance levels for the buckling and non-buckling problems, of classical primal approach, GIRKS-primal approach and direct sequential approach. The direct sequential solver requires 8667s to solve one linear system.

6.1 Non-buckling problem

As said before, this loading history leads to the computation of 48 linear systems with different matrices and right hand sides. The direct sequential approach is completed in 115h30min. Parallel performance results are given in table (2).

As can be seen, performance levels strongly depend on the choice of the decomposition though the number of subdomains is almost constant. Two factors justify these variations, first the heterogeneity of the interface (decompositions giving best results contain only mono-material substructures with different materials facing, while less efficient decompositions possess multi-materials interfaces with same materials facing), second the aspect ratio of substructures (due to the lower sparsity of matrices, massive substructures involve longer computation time for matrix manipulation).

k linear systems $(S^q u^q = b^q)_{q=1,\dots,k}$ were solved
for the $(q)^{th}$ linear system, we note
$W^q = \{w_0^q, \dots, w_{r^{q-1}}^q\}$ set of research directions
$r^q = \dim(W^q)$
$\Gamma^q = W^{qT} S^q W^q$ (diagonal matrix)
s^q ponderation term (most often 1)

Solution to the $(k+1)^{th}$ system

1. IRKS approach

1.1 Initialization

$\hat{u}_0 = G(G^T SG)^{-1} G^T b + P\chi$
$\hat{r}_0 = b - S\hat{u}_0$

1.2 Iterations $i = 0, \dots, p \ / \hat{z}_p = 0$

$$\hat{z}_i = P\left[\sum_{q=1}^{k} W^q \Gamma^{q-1} W^{qT}\right] \hat{r}_i$$

$$\hat{w}_i = \hat{z}_i + \sum_{j=0}^{i-1} \hat{\gamma}_{ij} \hat{w}_j \qquad (\hat{w}_0 = \hat{z}_0) \qquad \hat{\gamma}_{ij} = -\frac{(\hat{z}_i, S\hat{w}_j)}{(\hat{w}_j, S\hat{w}_j)}$$

$$\begin{array}{l|l} \hat{x}_{i+1} = \hat{x}_i + \hat{\alpha}_i \hat{w}_i & \\ \hat{r}_{i+1} = \hat{r}_i - \hat{\alpha}_i S\hat{w}_i & \hat{\alpha}_i = \frac{(\hat{r}_i, \hat{z}_i)}{(\hat{w}_i, S\hat{w}_i)} \end{array}$$

1.3 End of IRKS

$V = \{w_0, \dots, w_{p-1}\}$
$\Lambda = V^T SV$ (diagonal matrix)
$Q = Id - V\Lambda^{-1} V^T S$ projection matrix

2. Conjugate Gradient with GKC

2.1 Initialization

$x_0 = \hat{x}_{p+1}$
$r_0 = \hat{r}_{p+1}$

2.2 Iterations $i = 0, \dots, s$

$y_i = M^{-1} r_i$

Successive corrections $q = 1, \dots, k$

$$\tilde{r}_i^q = s_q W^q \Gamma^{q-1} W^{qT} r_i - W^q \Gamma^{q-1} W^{qT} S^q y_i^{q-1}$$
$$y_i^q = y_i^{q-1} + \tilde{r}_i^q$$

$z_i = QPy_i^k$

$$w_i = z_i + \sum_{j=0}^{i-1} \gamma_{ij} w_j \qquad (w_0 = z_0)$$

$$\begin{array}{l|l} x_{i+1} = x_i + \alpha_i w_i & \gamma_{ij} = -\frac{(z_i, Sw_i)}{(w_j, Sw_j)} \\ r_{i+1} = r_i - \alpha_i S w_i & \alpha_i = \frac{(r_i, z_i)}{(w_i, Sw_i)} \end{array}$$

Figure 1: Algorithm: GIRKS with Projected Preconditioned Conjugate Gradient

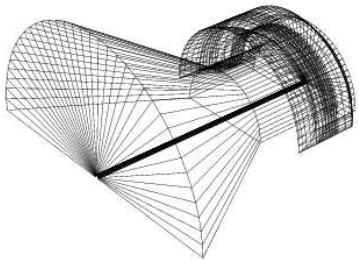

Figure 2: 3D view of flexible bearing

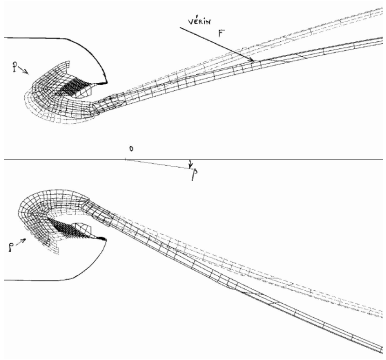

Figure 3: Axial view of reference and deformed structure

The turning stiffness (fig. 4) decreases when the pressure inside the booster increases, it can even become negative (the flexible bearing is then driving). This evolution, caused by the displacement of pieces, is properly simulated during the computation.

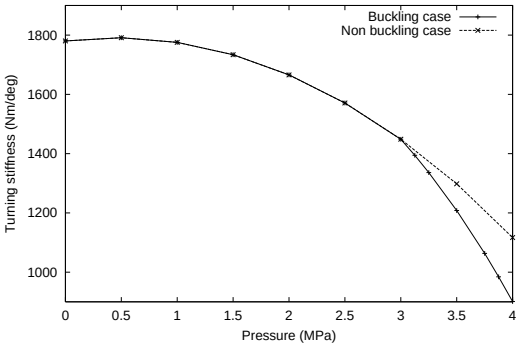

Figure 4: Turning stiffness

Problem		Aver. CPU time (s) / sys		It. nb	Gain
Decomposition	Method	Factorization	Total	Aver/sys	Seq./Par.
17a-1r (17 proc.)	Primal	14.5	140.7	164	**61.6**
17a-1r (17 proc.)	GIRKS	14.5	78	50	**111.1**
6a-3r (18 proc.)	Primal	22.4	412.8	398	**21**
6a-3r (18 proc.)	GIRKS	22.4	256.7	183	**33.7**
3a-6r (18 proc.)	Primal	144	939.2	362	**9.2**
3a-6r (18 proc.)	GIRKS	144	400.9	120	**21.6**

Table 2: Numerical performance Parallel/Sequential (non-buckling)

The Krylov acceleration strategy leads to significant speed-up. The CPU time, thanks to the use of GIRKS, increases from 38% to 58%. GIRKS enables to solve up to 111 times faster the non-linear problem than the sequential approach using only 17 processors.

Figures (9) and (10) respectively show the evolution of the average number of conjugate gradient iterations and the associated average CPU time to solve each linear system. Due to the very low cost of GIRKS, iterations and CPU time graphs are quite similar. As can be seen, the action of GIRKS grows as the nonlinear system number increases due to the increasing size of the stored Krylov subspaces. In the course of the non-linear resolution, it may occur that the information stored in Krylov subspaces becomes non-relevant and leads to a perturbation leading to stagnation. The linear resolution is then restarted with deletion of the stack of Krylov subspaces. The restarting procedure can be observed on figure (9) when two points are associated to the same linear system.

6.2 Buckling problem

This loading history leads to the computation of 37 linear systems with different matrices and right hand sides. The direct sequential approach is completed in 89h. The performance results of the parallel approaches are given in table (3). For the buckling problem, GIRKS is not as efficient as for the previous problem, but it still has a positive impact. The best result is then a resolution 67 times faster than the sequential approach using only 17 processors.

7 Conclusion

In this paper we considered the resolution of highly heterogeneous structures involving quasi-incompressible materials with a primal domain decomposition method. We extended the definition of scaling ma-

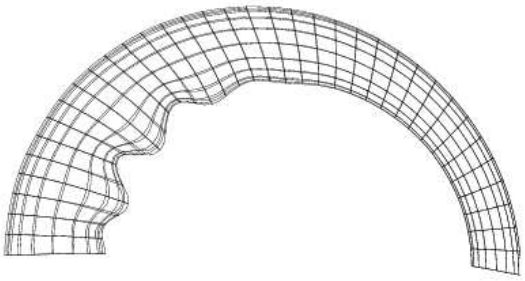

Figure 5: Buckling of one reinforcement

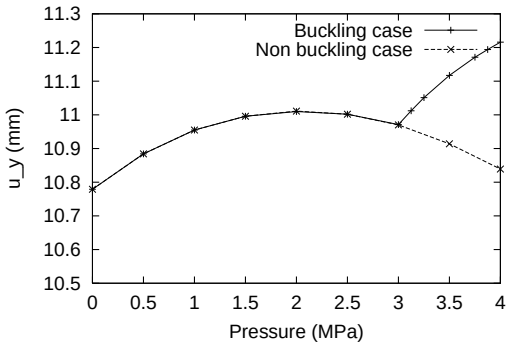

Figure 6: Radial displacement of an internal boundary point of a reinforcement

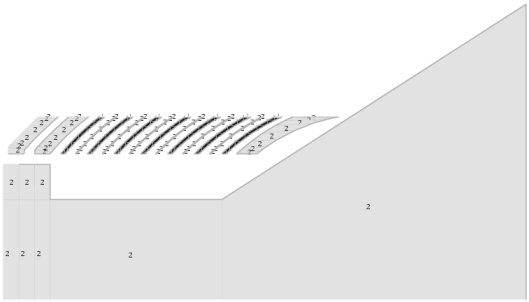

Figure 7: 17a decomposition

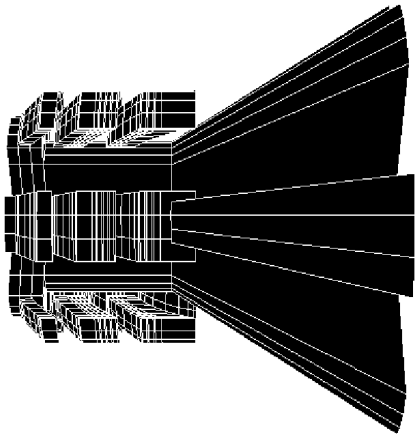

Figure 8: 3a-6r decomposition

Problem		Aver. CPU time (s) / sys		It. nb	Gain
Decomposition	Method	Factorization	Total	Aver/sys	Seq./Par.
17a-1r (17 proc.)	Primal	14.9	139	162	**62.3**
17a-1r (17 proc.)	GIRKS	14.9	130	102	**66.7**

Table 3: Numerical performance Parallel/Sequential (buckling)

trices to the case where pressure is condensed, restoring the scalability of the method to this class of problems. The resolution of the challenging assessment was successfully achieved using a Newton-Krylov approach. We showed that the reuse of Krylov subspaces with the GIRKS algorithm always lead to better performance, the speed-up compared to the classical primal approach can be 60%. Compared to the direct sequential approach, the resolution is conducted in the best case 111 times faster using only 17 processors. In order to avoid stagnation and restarting associated to GIRKS, we now develop new Krylov reuse strategies based on an exact coarse grid solver. Due to the significant computational cost of this new approach we couple it with a selective reuse of Krylov subspaces based on a spectral analysis of the linear systems [4].

Acknowledgements: The authors acknowledge support of computational resources by the Centre Informatique National Enseignement Supérieur and the Pôle de Calcul Paris Sud.

References

[1] Proceedings of the 14th international conference on domain decomposition methods, mexico, 2002.

[2] F. Brezzi and M. Fortin. *Mixed and hybrid finite element methods.* Springer series in Computational Mathematics, 1991.

[3] Charbel Farhat and François-Xavier Roux. Implicit parallel processing in structural mechanics. *Computational Mechanics Advances*, 2:1–24, 1994.

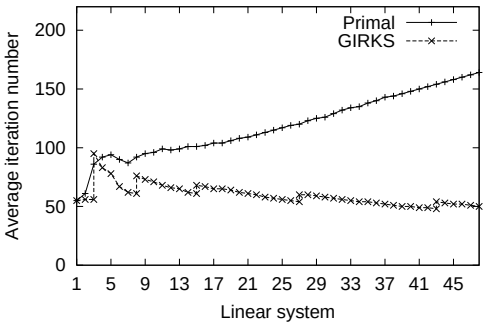

Figure 9: GIRKS: nb of iterations

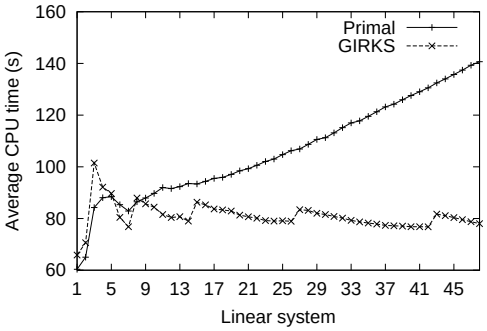

Figure 10: GIRKS: CPU time

[4] Pierre Gosselet and Christian Rey. On a selective reuse of krylov subspaces for newton krylov approaches in non-linear elasticity. In *14th international conference on domain decomposition methods*, Mexico, 2002.

[5] Julie Lambert-Diani and Christian Rey. New phenomenological behavior laws for rubbers and thermoplastic elastomers. *Eur. J. Mech. A/Solids*, 18:1027–1043, 1999.

[6] P. LeTallec. Domain decomposition methods in computational mechanics. In *Computational Mechanics Adv.*, volume 1. 1994.

[7] Patrick LeTallec. Numerical methods for non-linear three-dimensional elasticity. In Ciarlet PG and Lions JL., editors, *Handbook of numerical analysis*, volume 3. Elsevier, 1994.

[8] J. Mandel. Balancing domain decomposition. *Comm. Appl. Numer. Meth.*, 9:233–241, 1993.

[9] Christian Rey. Une technique d'accélération de la résolution de problèmes d'élasticité non-linéaire par décomposition de domaines. In *Comptes rendus de l'académie des sciences*, volume 322 of *II b*, pages 601–606. 1996.

[10] Christian Rey and Franck Risler. A rayleigh-ritz preconditioner for the iterative solution to large scale nonlinear problems. *Numerical Algorithms*, 17:279–311, 1998.

[11] Franck Risler and Christian Rey. Iterative accelerating algorithms with krylov subspaces for the solution to large-scale non-linear problems. *Numer. Algorithms*, 23:1–30, 2000.

[12] R.S. Rivlin and D.W. Saunders. Large elastic deformation of isotropic materials. experiments on the deformation of rubber. *Phil. Trans. Roy. Soc.*, A243:251–288, 1951.

[13] Daniel Rixen and Charbel Farhat. A simple and efficient extension of a class of substructure based preconditioners to heterogeneous structural mechanics problems. *Int. J. Num. Meth. Engrg.*, 44, 1999.

[14] Youssef Saad. On the lanczos method for solving symmetric linear systems with several right-hand sides. *Math. Comp.*, 48:651–662, 1987.